

AEOLIAN PROVINCES & ACTIVITY IN HERSCHEL CRATER, MARS. K. D. Runyon¹, N. T. Bridges², F. Ayoub³, S. Mattson⁴, ¹Johns Hopkins University Department of Earth & Planetary Sciences, Baltimore, MD, USA (kirby.runyon@jhuapl.edu), ²Applied Physics Laboratory, Laurel, MD, USA, ³Caltech, Pasadena, CA, USA, ⁴University of Arizona, Tucson, AZ, USA.

Introduction: Herschel crater (14.4°S, 130°E)—a degraded Noachian peak-ring basin almost 300 km in diameter located in the southern highlands—features multiple aeolian landforms (Fig. 1): barchan, barchanoid, and dome dune fields, numerous sand sheets, sand ripples, and indurated transverse aeolian ridges (TARs). It thus serves as a natural laboratory for studying dune & ripple migration rates & direction, sediment flux, deposition & erosion rates, sediment sources and sinks, bedform induration, and generally the evolution of a landscape as caused by wind-mobilized sediment over most of Mars' geologic history. Distinguishing Herschel among other bedform-filled basins are 1) Complex ripple patterns [1]; 2) Proximity to Gale crater (~700 km SW of MSL's landing site) and thus the ability to make inferences about Gale from Herschel; and 3) More diverse aeolian geomorphologies compared to sites such as Nili Patera [2].

Wind mobilizes sediment in four principle ways, which each contribute to the total aeolian sediment flux: saltation, reptation, creep, and suspension [e.g. 3, 4]. Saltation drives bulk dune formation and movement whereas reptation (grain splash from saltation) drives ripple formation and movement [5]. As dunes, ripples, and their changes are highly visible in HiRISE images, they naturally lend themselves to this study of bedforms and sand fluxes within Herschel crater.

Here, we report on progress measuring ripple migration on dunes and sand sheets, as well as dune slip face advancement. We estimate the corresponding sand fluxes and consider the broader geologic and atmospheric implications in Herschel crater and elsewhere.

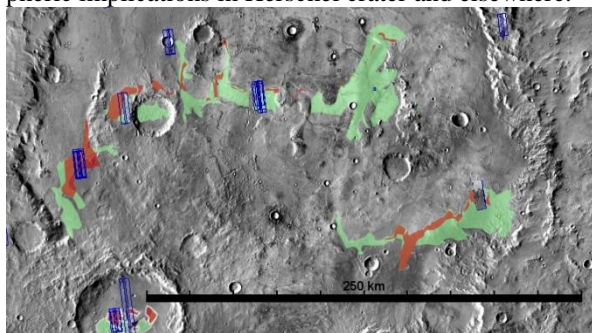


Fig. 1. THEMIS mosaic of Herschel crater, where barchan and dome dune fields are mapped in red and the darkest aeolian deposits—commonly sand sheets—are mapped to light green. Note that generally dune fields grade downwind into sand sheets. Not mapped are small features commonly in the crater's north interpreted as transverse aeolian ridges (wavelengths of a few 10s of m), appearing to be indurated and with superposing craters. Blue outlines denote HiRISE images. Mapped in JMARS [6].

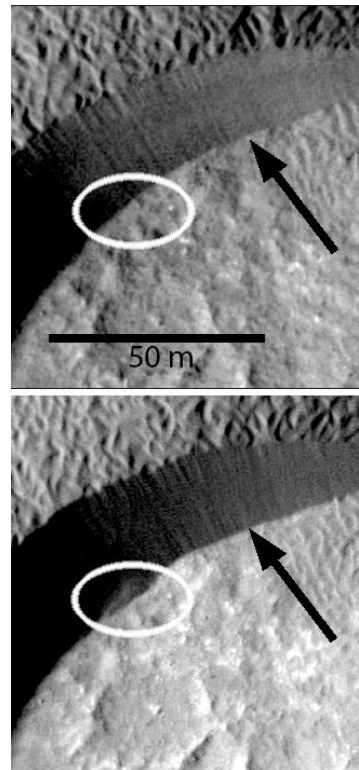


Fig. 2. Slip face advance spanning 3.74 Earth years shown by arrow. Slip face grain flow event illustrated in oval. PSP_002860-1650 & ESP_020384_1650.

Methods:

HiRISE repeatedly imaged three aeolian provinces within Herschel, termed here as Herschel West, Herschel Center, and Herschel East. Stereo HiRISE imagery allowed for the production of DEMs [7,8], orthoimagery, and automated ripple change detection [9] between images at two of the three sites. We used rip-

ple displacement to estimate sand flux from reptation. To measure dune lee front advance rate we mapped slip faces on two co-registered images, using the method of [11,12]. Multiplying this rate by the dune height yielded total bulk sand flux = saltation + reptation + creep.

To obtain the contribution to total flux from reptation, we used the ENVI module Co-registration of Optically Sensed Images and Correlation (COSI-Corr; [9]) to 1) create sub-pixel, co-registered orthoimages; and 2) extract a ripple displacement map by automatically tracking the movement of ripple patterns (Fig. 4). Defining transects along dunes' long axes allowed extraction of both ripple displacement and dune height. The overall procedure is identical to that used by [2].

Results: Presented in Table 1, we report bedform migration rates, the corresponding sand fluxes (in bold), and the above-threshold wind azimuth. Fig. 3 shows a unidirectional NW wind azimuth derived from the ripple migration (Fig. 4) for both Herschel West and Center.

Table 1. Ripple half-heights used in flux calculations for Herschel West & Herschel Center are 15 cm and 17.5 cm, respectively. Bold labels denote sand fluxes rather than migration rates. Underlined values are used in calculating the ratio of reptation/total migration.

	West (Dunes)	Center (Sand Sheets)	East (Dunes)
Mean ripple migration rate (m/yr)	$0.41 \pm 0.07\sigma$	$0.83 \pm 0.2\sigma$	<i>Insufficient Data</i>
Reptation Sand Flux at Dune Crest ($m^3/m/yr$)	$4.4 \pm 2.5\sigma$	<i>No dunes</i> (ripple flux = $0.15 \pm 0.04\sigma$)	<i>Insufficient Data</i>
Dune migration rate from reptation (m/yr) (ripple displacement*ripple half height/(dune height*time)	<u>$0.063 \pm 0.093\sigma$</u>	<i>No dunes</i>	<i>Insufficient Data</i>
Lee advance rate (m/yr)	<i>Insufficient Data</i>	<i>No dunes</i>	$0.4 \pm 0.1\sigma$
Total Flux (Rep. + Salt.) ($m^3/m/yr$)	<i>Insufficient Data</i>	-	$7.5 \pm 2.6\sigma$
Ratio of migration rates: rep/(rep+salt+creep)	(West reptation dune migration/East total migration) = <u>0.16 ± 0.03</u>		
Ave. Wind Azimuth above Saltation Threshold	$330^\circ \pm 6\sigma$	$342^\circ \pm 12\sigma$	$\sim 20^\circ$

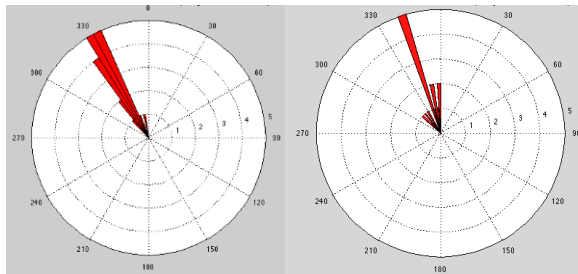


Fig. 3. *Left:* Herschel West showing northwest-to-southeast wind azimuth as indicated from ripple migration trajectories on dunes. *Right:* North-northwest to south-southeast wind azimuth for Herschel Center. The rose diagrams are binned in 4° increments. Unidirectional winds are expected for well-developed barchan dune fields such as in Herschel crater.

In Herschel East, there is currently insufficient repeat imagery to form a DEM and therefore a ripple displacement map. However, using the two images spanning over six Earth years, slip face advancement and bulk dune sand fluxes were estimated by measuring the ground-projected width of slip faces and estimating their height assuming a slip face angle of 33° [3]. We summarize the total sand flux from Herschel East in Table 1 and also compare it to the reptation-only effects from Herschel West, showing that reptation-only effects are $\sim 16\%$ to the total bedform migration rate. Future work measuring slip face advancement in Herschel West will enable us to compare reptation-only migration and bulk migration on the same dunes.

Estimates of total sand flux for Herschel Center are currently hampered due to extensive sand sheets and lack of dune slip faces. Measuring total sand flux will require using the center-of-figure method from [12].

Discussion & Conclusion: Assuming that all dune migration is from reptation, [2] reports rates in Nili Patera that are 20% of total dune migration as measured from slip face advancement. Combining Herschel East total dune migration rates with Herschel West reptation-only dune migration rates, we find a similar value of 16%.

Table 1 shows that ripple migration rates for Herschel West and Center ranged from 0.41-0.83 m/yr, bracketing a similar value for [13]'s value of 0.66 m/yr for Gale crater ripples. These consistent results contrast to [2]'s much faster ~ 5 m/yr Nili Patera ripples.

The unidirectional winds evidenced by bedforms can constrain GCMs to exclude winds of high shear stress (i.e. fast enough to initiate saltation) in directions other than those directly measured. The indurated TARs point to a similar paleowind direction, namely \sim north-to-south.

Future work will include deriving total sand fluxes in Herschel West and better comparisons of West and East to Herschel Center; comparisons to detailed investigations ongoing in Nili Patera; hypothesizing on possible sediment sources and sinks; and hypothesizing on Herschel's curiously irregular ripple patterns.

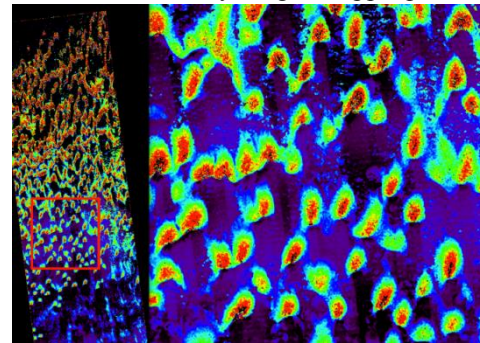


Fig. 4. Ripple displacement map of barchan and dome dune field in Herschel West. The right side shows an enlargement of the boxed region on the left. Warmer colors denote greater displacements. The image at left is ~ 5 km wide. Correlation between HiRISE images PSP_002860_1650 & ESP_020384_1650.

References: [1] Bridges et al., (2012), *Geology*, v. 40, no. 1, p. 31-34. [2] Bridges N. T. et al. (2012) *Nature* 485, 339, doi:10.1038/nature11022. [3] Bagnold R. A. (1941) *Dover 0-486-43931-3*. [4] Kok J. F. et al. (2012) *Rep. Prog. Phys.* 75, 106901. [5] Anderson, R.S. (1987) *Sedimentology* v. 34, no. 5, p. 943-956, doi: 10.1111/j.1365-3091.1987.tb00814.x [6] JMARS (2013), jmars.asu.edu. [7] Kirk, R. et al. *7th International Conf. Mars*, 3381 Pasadena, CA (2008). [8] Mattson, S. et al., (2009), *European Planetary Science Congress, EPSC2009-604*. [9] Leprince S. et al., (2007) *IEEE Trans. Geosci. & Rem. Sensing*, 45, 6. [10] Hansen C.J. et al. (2011) *Science*, v. 331, p. 575-578. [12] Bridges et al., (2013) *Aeolian Research*, 9, p. 133-151. [13] Silvestro et al. (2013) *Geology*, v. 41, no. 4, p. 483-486, doi:10.1130/G34162.1.